CHAPTER V

PREPARATION AND CHARACTERIZATION OF GRAPHENE OXIDE/TIN OXIDE NANOCOMPOSITES AS COUNTER ELECTRODE IN DYE SENSITIZED SOLAR CELL

5.1 INTRODUCTION

Dye sensitized solar cells (DSSC) are promising candidates for low cost and clean energy conversion devices. DSSC is a third generation solar cell technology that has been widely investigated in view of its ease of fabrication, low cost of production, and eco-friendly nature, providing photovoltaic efficiency. DSSCs are usually composed of a dye coated crystalline semiconductor coated on a transparent conductive oxide, an electrolyte and a counter electrode [1]. The most commonly employed material as counter electrode in DSSCs is platinum due to its excellent catalytic, thermal and electrical properties with considerable low charge transfer resistance. However, high cost associated with Pt is a hurdle towards commercialization for large scale production. Currently researchers are therefore in constant search of alternative electrode materials with sufficient efficiency to replace Pt based DSSC. Hence an attempt is made to use Graphene oxide / Tin oxide as a counter electrode [2].

Graphene, a two dimensional one atom thick sheet of sp^2 hybridized carbon atoms that have been expected to be the most promising alternative to Pt, due to its excellent electrical, catalytic and mechanical properties. These properties make graphene oxide as an excellent electrode material for the electrochemical applications. SnO_2 nanoparticles are a highly significant group of materials with applications in gas sensors, transparent conducting electrodes, and transistors [3]. Because of the optical conduction of SnO_2 nanoparticles, this has recently been extended to solar cells. SnO_2 can bond to the surface of graphene thereby increasing the mechanical stability of the graphene oxide nanosheet and also potentially improves the photovoltaic performance of DSSCs [4].

5.2. MATERIAL AND EXPERIMENTS

5.2.1 Materials

Graphene oxide is prepared using modified Hummers' method. Tin oxide (SnO_2) are purchased from Sigma Aldrich and used without further purification.

5.2.2. Synthesis of GO/SnO_2Nanocomposites

Graphene oxide nanosheet are synthesized by modified Hummers' method. Graphene oxide/ Tin oxide (GO/SnO_2) nanocomposites are synthesized by simple chemical method. 100 mg of graphene oxide is dissolved in 60 ml of distilled water and are sonicated for 1 hour, followed by the addition of SnO_2 into the dispersed solution and are kept under stirring for 7 hours at 60ºC. This homogeneous solution is kept for 12 hours at room temperature and the products are separated by centrifugation and are washed with deionized water for several times, dried at 80ºC for 5 hours and are grinded to fine powder [5].

5.2.3 Characterization Techniques

The crystalline structure of the prepared GO nanosheet is characterized using X'PERT^3 Panalytical Diffractometer. The FT-IR spectrum is recorded for the presence of the nanosheet using Shimadzu IR affinity-1. Raman spectra are recorded at ambient temperature on a Nano Tech 1 (QEB0120) model. The morphology and microstructure of the sample are studied using field emission scanning electron microscopy (FESEM) using ZEISS-SIGMA and high resolution transmission electron microscopy (HR-TEM) using Jeol JEM 2100. The elemental composition is tested using Energy Dispersive X-ray Spectroscopy (EDX).

5.3. RESULTS AND DISCUSSION

5.3.1 XRD Analysis

X-ray diffraction of the synthesized nanocomposites are carried out in order to investigate the structural and crystalline nature of SnO_2 and GO/SnO_2(5:1, 5:2, 5:3 5:4 and 5:5). Figure 5.1 (a) represents the diffraction peaks positioned at 2θ values of 26.79º, 34.59º, 38.69º, 51.42º and 54.70ºthat corresponds to the (110), (101), (200), (221) and (220) planes respectively and are well matched with the JCPDS card no 41-

1445, which confirms the formation of SnO_2nanoparticles [6]. The crystallite size of $SnO_2$is found to be around 20 nm.

Figure 5.1 (b-f) shows the peaks appeared at 2θvalues of11.39º, 26.79º, 34.59º, 38.69º, 51.42º and 54.70º that corresponds to (002), (110), (101), (200), (221) and (220) planes respectively which confirms the formation of GO/SnO_2 nanocomposites. It is observed from XRD analysis that the intensity of the diffraction peaks of nanocomposites increases with increase in SnO_2 concentrations of 5:1, 5:2, 5:3, 5:4 and 5:5. It is also observed for the diffraction peak of Graphene oxide 11.39º, the intensity decreases after the embellishment of SnO_2 nanoparticles on the Graphene oxide surface [7]. The crystallite size of GO/SnO_2 (5:1, 5:2, 5:3, 5:4 and 5:5) nanocomposites are calculated using Debye Scherrer and are found to be 22.3 nm, 23.1nm, 24.5 nm, 25.2 and 25.9 nm respectively. The increases in the crystallite size may be due to increases in the SnO_2 concentration on the surface of GO nanosheet. No impurity peak is observed from XRD analysis and also confirmed from EDAX analysis.

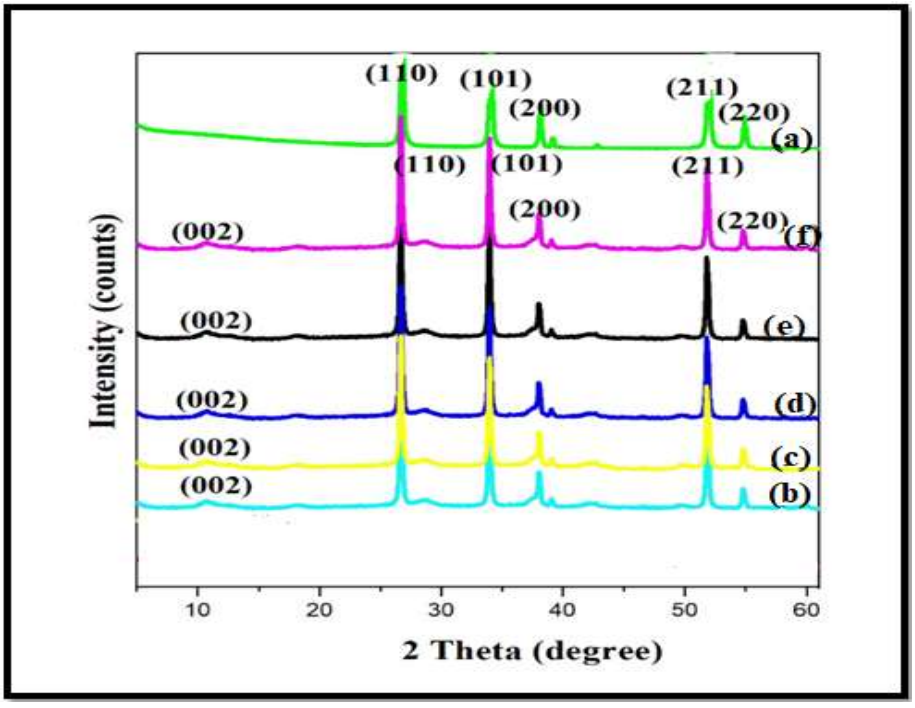

Figure 5.1 XRD Spectra of (a) SnO_2 (b-f) GO/SnO_2 (5:1, 5:2, 5:3, 5:4 and 5:5) nanocomposites

5.3.2 FT-IR Spectral Analysis

The nature of chemical groups and deoxygenating degree of oxygen functional groups in GO and SnO_2nanocompositesare characterized using Fourier Transform Infrared (FT-IR) spectrum. Figure 5.2 (a-f) shows the FT-IR spectra of prepared SnO_2 and GO/SnO_2 (5:1, 5:2, 5:3, 5:4 and 5:5) nanocomposites. Figure 5.2 (a) shows the FT-IR spectrum ofSnO_2 nanoparticles and bands are depicted at 660 cm^{-1} and 520 cm^{-1} represents Sn-O vibrations thereby confirming the formation of SnO_2 nanoparticles. Figure 5.2 (b-f) shows that the bands appeared at 3653 cm^{-1} and 1590 $cm^{-1}$are corresponding to the stretching and bending vibrational modes of O-H respectively and the band at 662 cm^{-1} and 505 cm^{-1} is due to Sn-O vibration that confirms the successful formation of SnO_2 and GO/SnO_2 (5:1, 5:2, 5:3, 5:4 and 5:5) nanocomposites. These results reveal the abundance of hydroxyl groups on the surface of GO nanosheet and the peak around 1185 cm^{-1} is attributed to C-H bending vibration of the nanocomposites. The symmetric stretching at 660 cm^{-1} and Sn-O asymmetric stretching at 530 cm^{-1} in GO/SnO_2 (5:1, 5:2, 5:3, 5:4 and 5:5) as opposed to that of GO establish the successful incorporation of SnO_2 nanoparticles in Graphene Oxide nanosheet [8].

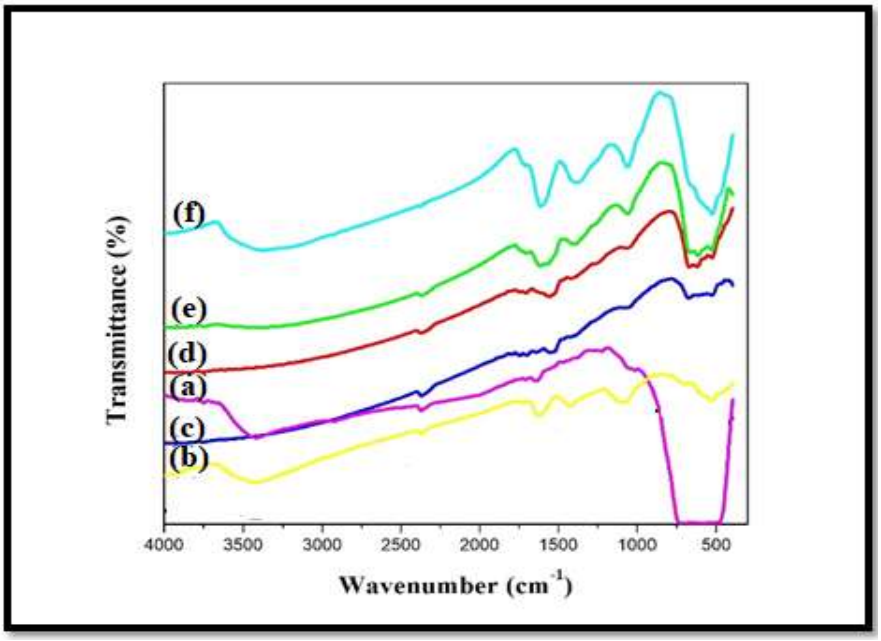

Figure 5.2 FT-IR Spectrum of (a) SnO_2 and (b-f) GO/SnO_2 (5:1, 5:2, 5:3, 5:4 and 5:5) nanocomposites

5.3.3 Raman Spectral Analysis

Figure 5.3 show the Raman Scattering spectroscopy of SnO_2 and GO/SnO_2 (5:1, 5:2, 5:3, 5:4 and 5:5) nanocomposites. The significant structural changes are occurred during chemical processing from GO to GO/$SnO_2$and are also reflected in the Raman spectra. SnO_2 nanoparticles show broad peaks at 632.60 cm^{-1} and 766.88 cm^{-1} and are due to the Sn-O stretching mode [9]. Figure 5.3 (a-f) shows three noticeable peaks around 660.59 cm^{-1}, 1342.9 cm^{-1} and 1606.17cm^{-1}, which confirms the presence of GO and SnO_2 nanocomposites. The GO and SnO_2 peaks have slight shift due to increase in the concentration (5:1, 5:2, 5:3, 5:4 and 5:5) of SnO_2 nanoparticles on the surface of Graphene oxide nanosheet. It is evident that the Raman results are consistent with XRD results, indicating the formation of GO/SnO_2nanocomposites [10].

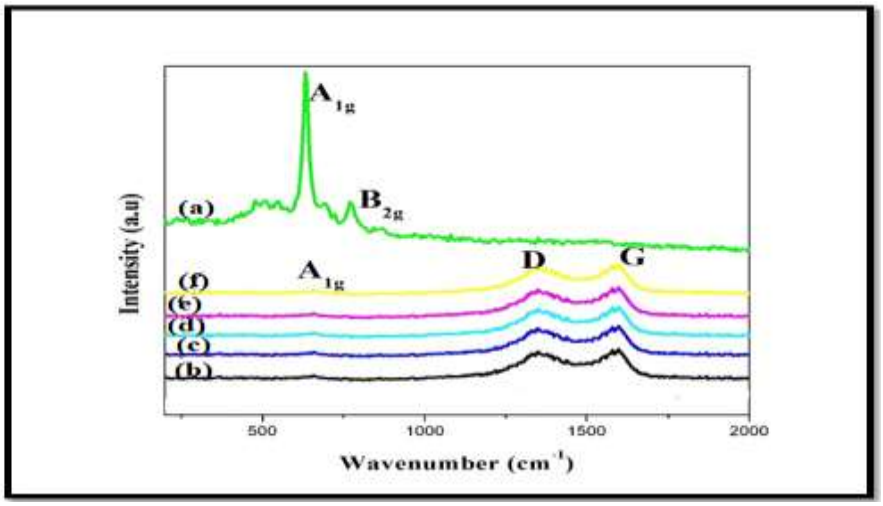

Figure 5.3 (a-e) Raman analysis of (a) SnO_2 (b-f) GO/SnO_2 (5:1, 5:2, 5:3, 5:4 and 5:5) nanocomposites

5.3.4. FESEM

Field emission scanning electron microscopy (FESEM) analysis is performed to study the surface morphology and the shape of prepared nanocomposites. Figure 5.4 (a-f) shows the FESEM images of the prepared SnO_2 and GO/SnO_2 (5:1, 5:2, 5:3, 5:4 and 5:5) nanocomposites. It is observed from the Figure 5.4 (a) that the prepared SnO_2 has spherical shape with diameter in the range of 30 nm. Figure 5.4 (c-e) shows the FESEM images of various concentrations (5:1, 5:2, 5:3, 5:4 and 5:5) of SnO_2 nanoparticles decorated on the graphene oxide nanosheet. It is observed that SnO_2

nanoparticles are deposited evenly on the curled and wrinkled surface of the graphene oxide sheet, indicating the immobilization effect of the graphene sheet and good amalgamation between graphene sheets and SnO_2 nanoparticles. FESEM analysis also confirms that 5:5 concentrations of SnO_2 nanoparticles are highly blended on the large surface area of graphene oxide nanosheet [11].

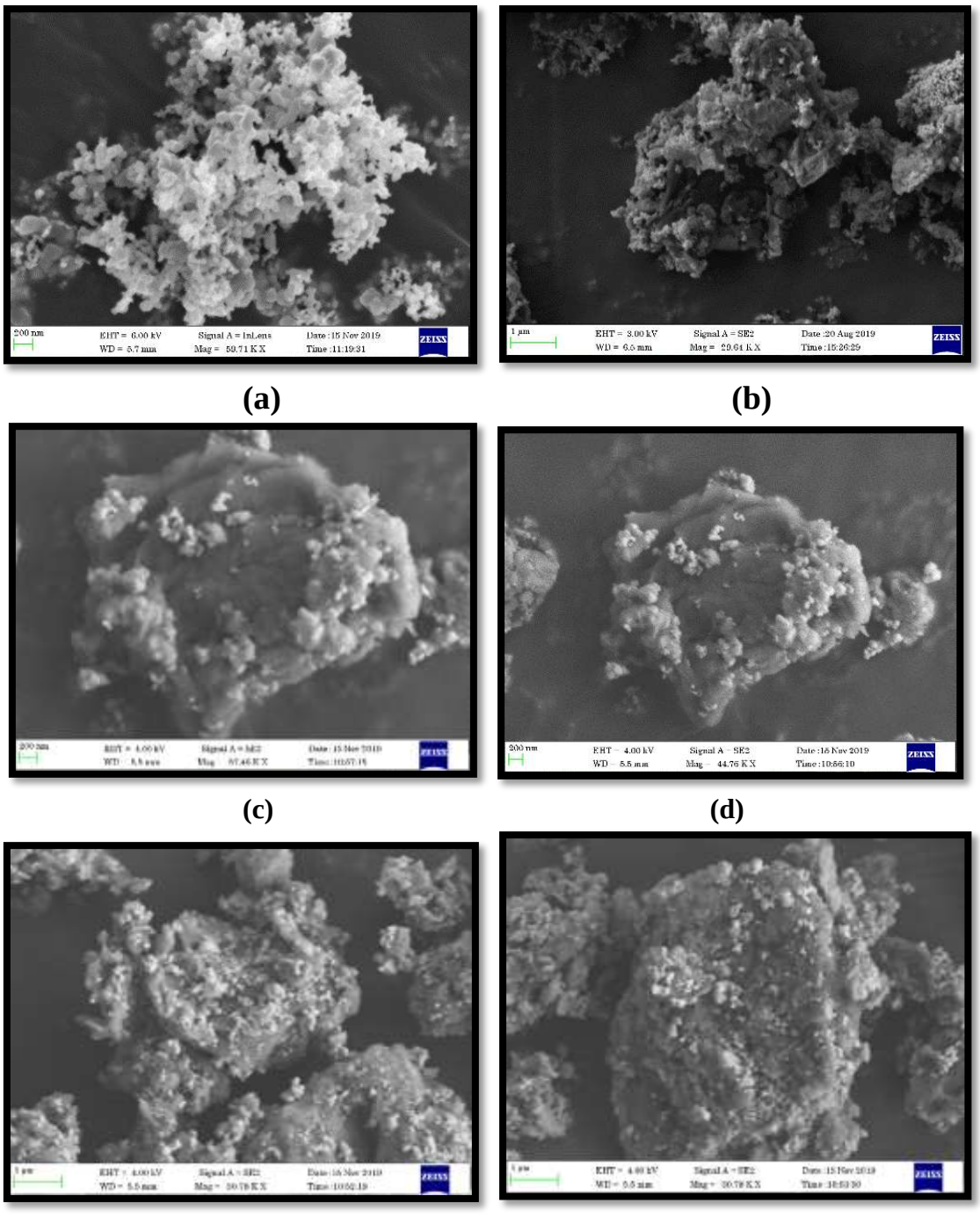

(a) **(b)**

(c) **(d)**

(e) **(f)**

Figure 5.4 FESEM (a) SnO_2 and (b-f) GO/SnO_2 (5:1, 5:2, 5:3, 5:4 and 5:5) nanocomposites

5.3.5 EDX Analysis

The EDX analysis is used to identify the elemental presence in the prepared nanocomposites. Figure 5.5 (a-e) represents the EDX spectra of SnO_2 and GO/SnO_2 (5:1, 5:2, 5:3, 5:4 and 5:5) nanocomposites. Figure 5.5 (a) shows that the presence of Sn and O elements without any impurities. Figure 5.5 (c-e) shows the presence of C, O and Sn that confirms the formation of GO/SnO_2 (5:1, 5:3 and 5:5) with the atomic and weight percentage are given as inset table. The atomic percentage of SnO_2 in 5:1, 5:2, 5:3, 5:4 and 5:5 concentrations are 14.9%, 18%, 27%, 31% and 34.49% respectively. It is also confirmed from EDX analysis that with increase in the concentration of SnO_2 from 5:1 to 5:5, the number of SnO_2 atoms increases on the surface of GO nanosheet and further evidenced from SnO_2 atomic percentage provided in the inset table. The presence of SnO_2 atoms on the surface of GO increases is further confirmed from the FESEM analysis [12].

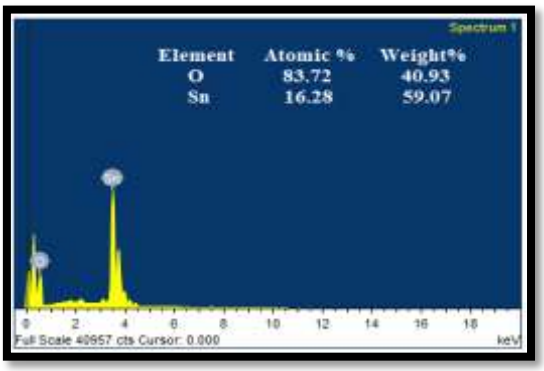

(a)

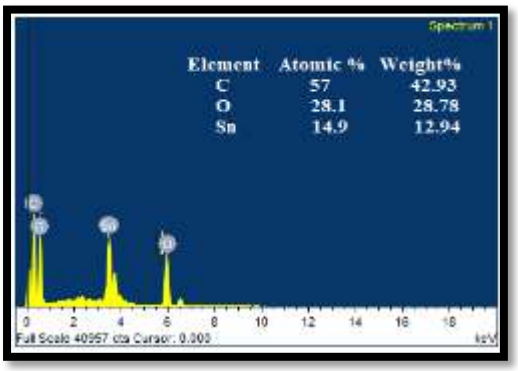

(b)

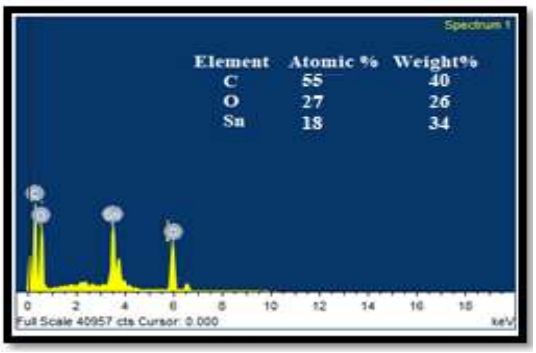

(c)

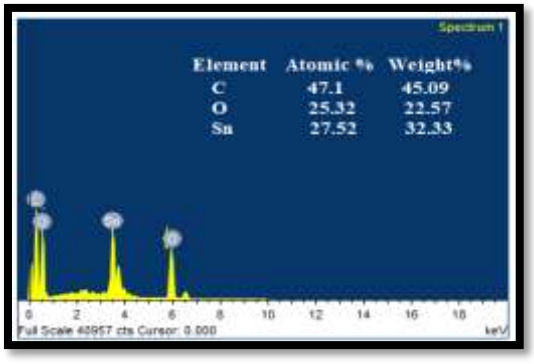

(d)

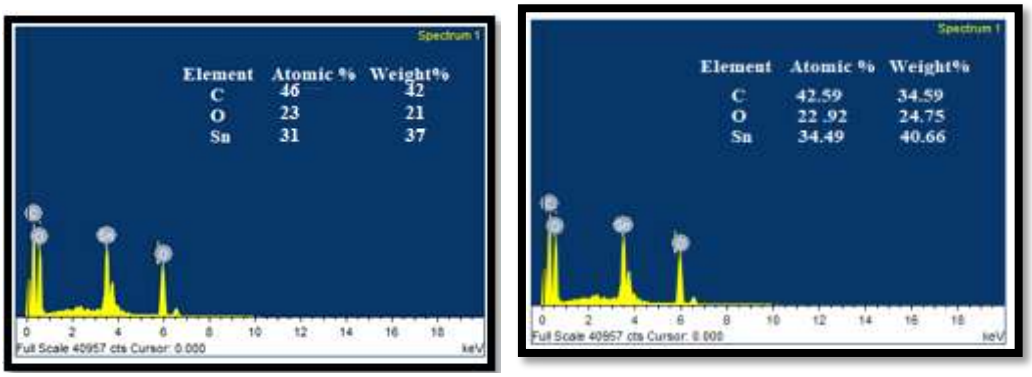

(e) **(f)**

Figure 5.5 EDAX Spectra (a) GO (b) SnO_2 (c-e) GO/SnO_2 (5:1, 5:2, 5:3, 5:4 and 5:5) nanocomposites

5.3.6 HR-TEM

Figure 5.6 (a-c) shows the HR-TEM images of GO/SnO_2 (5:5) nanocomposites. HR-TEM images of GO/SnO_2 (5:5) nanocomposites show the wide distribution of particles ranging in the diameter of 25 nm. The SnO_2 nanoparticles are distributed uniformly on the graphene nanosheet which prohibits the graphene nanosheet from aggregating. It is further observed from the Figure 5.6 that the spherical shape of SnO_2 nanoparticles are equally blended on the surface of GO nanosheet [13].

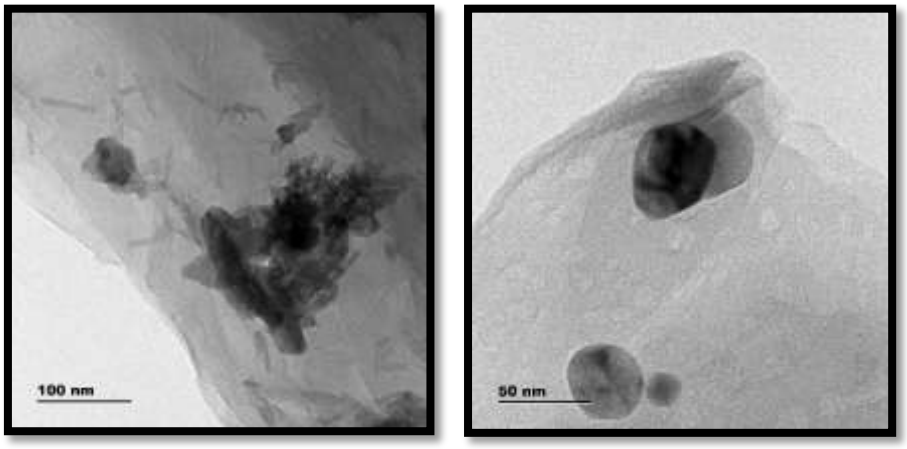

(a) **(b)**

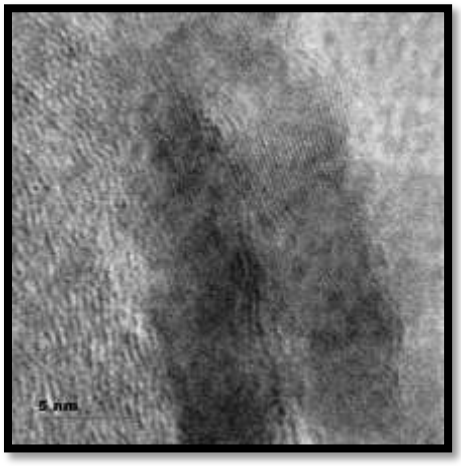

(c)

Figure 5.6 HR-TEM images of (a-c) GO/SnO_2 (5:5) nanocomposites

5.3.7 Selected Area Electron Diffraction

The Selected area electron diffraction pattern (SEAD) of the prepared nanocomposites GO/SnO_2 (5:5) is shows in the Figure 5.7. The SAED results shows that the five spotted ring that are consistent with the XRD patterns of GO/SnO_2 (5:5) and each rings corresponds to the (002), (110), (101), (200) and (211) planes of GO/SnO_2 nanoparticles, which could also be evidenced from XRD analysis [14,15].

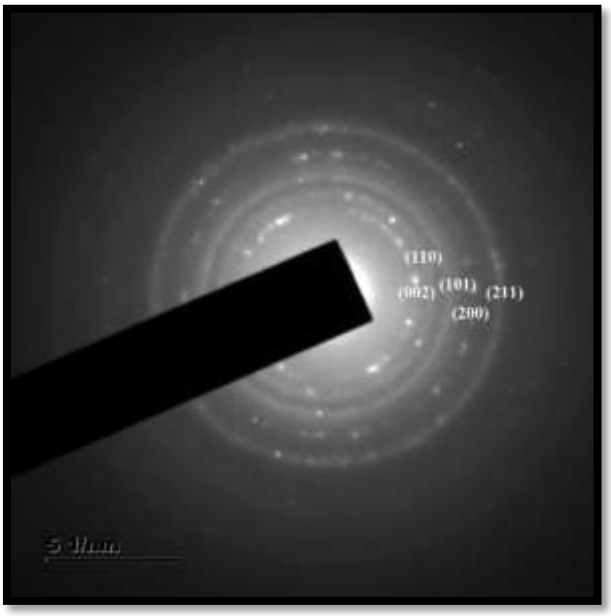

Figure 5.7 SAED image of GO/SnO_2 (5:5) nanocomposites

5.4. CONCLUSION

This chapter describes the GO/SnO_2 (5:1, 5:2, 5:3, 5:4 and 5:5) nanocomposites prepared by chemical precipitation method. XRD analysis showed that the prepared nanocomposites are crystalline in nature and the average crystallite size of GO/SnO_2 (5:1, 5:2, 5:3, 5:4 and 5:5) nanocomposites is found to be 22.3 nm, 23.1 nm, 24.5 nm, 25.2 and 25.9 nm respectively. FE-SEM and HR-TME analysis revealed that the SnO_2 nanoparticles are successfully embellished on the Graphene oxide nanosheet. The elemental analysis confirmed that the different concentrations of SnO_2 nanoparticles and Graphene oxide elements in the prepared nanocomposites are present without any impurities. This prepared nanocomposite entitled to use as a counter electrode for Pt Free Dye sensitized solar cell application.

REFERENCES

1. P. Wang, S. M. Zakeeruddin, I. Exnar, and M. Gratzel, Chem. Commun. , 2972 (2002).
2. X. X. Zhang, C. F. Deng, R. Xu, and D. Z. Wang, Journal of Materials Science 42, 8377 (2007).
3. Z. Li, G. Su, X. Wang, and D. Gao, Solid State Ionics 176, 1903 (2005).
4. M. Forsyth, Solid State Ionics 147, 203 (2002).
5. A. M. Stephan and K. Nahm, Polymer 47, 5952 (2006).
6. J. Zhang, H. Han, S. Wu, S. Xu, C. Zhou, Y. Yang, and X. Zhao, Nanotechnology 18, 295606 (2007).
7. W. S. Chi, D. K. Roh, S. J. Kim, S. Y. Heo, and J. H. Kim, Nanoscale 5, 5341 (2013).
8. J. Zhang, H. Han, S. Wu, S. Xu, Y. Yang, C. Zhou, and X. Zhao, Solid State Ionics 178, 1595 (2007).
9. G. Katsaros, T. Stergiopoulos, I. Arabatzis, K. Papadokostaki, and P. Falaras, Journal of Photochemistry and Photobiology A: Chemistry 149, 191 (2002).
10. P. Wang, S. M. Zakeeruddin, P. Comte, I. Exnar, and M. Grätzel, Journal of the American Chemical Society 125, 1166 (2003), pMID: 12553808, https://doi.org/10.1021/ja029294+ . 208 209
11. X. Zhang, H. Yang, H.-M. Xiong, F.-Y. Li, and Y.-Y. Xia, Journal of Power Sources 160, 1451 (2006), special issue including selected papers presented at the International Workshop on Molten Carbonate Fuel Cells and Related Science and Technology 2005 together with regular papers.
12. Y. GENG, X. SUN, Q. CAI, Y. SHI, and H. LI, Rare Metals 25, 201 (2006).
13. Y.-C. Wang, K.-C. Huang, R.-X. Dong, C.-T. Liu, C.-C. Wang, K.-C. Ho, and J.-J. Lin, J. Mater. Chem. 22, 6982 (2012).
14. O. Byrne, I. Ahmad, P. K. Surolia, Y. K. Gunko, and K. R. Thampi, Solar Energy 110, 239 (2014).
15. K. Prabakaran, A. K. Palai, S. Mohanty, and S. K. Nayak, RSC Advances 5, 66563 (2015).